Modeling of TeV Galactic Cosmic-ray Anisotropy based on Intensity Mapping in an MHD Model Heliosphere

M. Amenomori[1], Y. W. Bao[2], X. J. Bi[3], D. Chen[4], T. L. Chen[5], W. Y. Chen[3], Xu Chen[4], Y. Chen[2], Cirennima[5], S. W. Cui[6], Danzengluobu[5], L. K. Ding[3], J. H. Fang[3,7], K. Fang[3], C. F. Feng[8], Zhaoyang Feng[3], Z. Y. Feng[9], Qi Gao[5], Q. B. Gou[3], Y. Q. Guo[3], Y. Y. Guo[3], Y. Hayashi[10], H. H. He[3], Z. T. He[6], K. Hibino[11], N. Hotta[12], Haibing Hu[5], H. B. Hu[3], K. Y. Hu[3,7], J. Huang[3], H. Y. Jia[9], L. Jiang[3], P. Jiang[4], H. B. Jin[4], K. Kasahara[13], Y. Katayose[14], C. Kato[10], S. Kato[15], I. Kawahara[14], T. Kawashima[15], K. Kawata[15], M. Kozai[16], Labaciren[5], G. M. Le[17], A. F. Li[3,9,18], H. J. Li[5], W. J. Li[3,9], Y. Li[4], Y. H. Lin[3,7], B. Liu[19], C. Liu[3], J. S. Liu[3], L. Y. Liu[4], M. Y. Liu[5], W. Liu[3], H. Lu[3], T. Makishima[14], Y. Masuda[10], S. Matsuhashi[14], M. Matsumoto[10], X. R. Meng[5], Y. Meng[3,7], A. Mizuno[15], K. Munakata[10], Y. Nakamura[15], H. Nanjo[1], C. C. Ning[5], M. Nishizawa[20], R. Noguchi[14], M. Ohnishi[15], S. Okukawa[14], S. Ozawa[21], X. Qian[4], X. L. Qian[22], X. B. Qu[23], T. Saito[24], M. Sakata[25], T. Sako[15], T. K. Sako[15], T. Sasaki[11], J. Shao[3,9], T. Shibasaki[26], M. Shibata[14], A. Shiomi[26], H. Sugimoto[27], W. Takano[11], M. Takita[15], Y. H. Tan[3], N. Tateyama[11], S. Torii[28], H. Tsuchiya[29], S. Udo[11], R. Usui[14], H. Wang[3], S. F. Wang[5], Y. P. Wang[5], Wangdui[5], H. R. Wu[3], Q. Wu[5], J. L. Xu[4], L. Xue[8], Z. Yang[3], Y. Q. Yao[4], J. Yin[4], Y. Yokoe[15], Y. L. Yu[3,7], A. F. Yuan[5], L. M. Zhai[4], H. M. Zhang[3], J. L. Zhang[3], X. Zhang[2], X. Y. Zhang[8], Y. Zhang[3], Yi Zhang[30], Ying Zhang[3], S. P. Zhao[3], Zhaxisangzhu[5], X. X. Zhou[9], Y. H. Zou[3,7], and N. V. Pogorelov[31]

[1]Department of Physics, Hirosaki University, Hirosaki 036-8561, Japan.
[2]School of Astronomy and Space Science, Nanjing University, Nanjing 210093, China.
[3]Key Laboratory of Particle Astrophysics, Institute of High Energy Physics, Chinese Academy of Sciences, Beijing 100049, China.
[4]National Astronomical Observatories, Chinese Academy of Sciences, Beijing 100101, China.
[5]Department of Mathematics and Physics, Tibet University, Lhasa 850000, China.
[6]Department of Physics, Hebei Normal University, Shijiazhuang 050016, China.
[7]University of Chinese Academy of Sciences, Beijing 100049, China.
[8]Institute of Frontier and Interdisciplinary Science and Key Laboratory of Particle Physics and Particle Irradiation (MOE), Shandong University, Qingdao 266237, China.
[9]Institute of Modern Physics, SouthWest Jiaotong University, Chengdu 610031, China.
[10]Department of Physics, Shinshu University, Matsumoto 390-8621, Japan.
[11]Faculty of Engineering, Kanagawa University, Yokohama 221-8686, Japan.
[12]Faculty of Education, Utsunomiya University, Utsunomiya 321-8505, Japan.
[13]Faculty of Systems Engineering, Shibaura Institute of Technology, Omiya 330-8570, Japan.

[14]Faculty of Engineering, Yokohama National University, Yokohama 240-8501, Japan.
[15]Institute for Cosmic Ray Research, University of Tokyo, Kashiwa 277-8582, Japan.
[16]Polar Environment Data Science Center, Joint Support-Center for Data Science Research, Research Organization of Information and Systems, Tachikawa 190-0014, Japan.
[17]National Center for Space Weather, China Meteorological Administration, Beijing 100081, China.
[18]School of Information Science and Engineering, Shandong Agriculture University, Taian 271018, China.
[19]Department of Astronomy, School of Physical Sciences, University of Science and Technology of China, Hefei 230026, China.
[20]National Institute of Informatics, Tokyo 101-8430, Japan.
[21]National Institute of Information and Communications Technology, Tokyo 184-8795, Japan.
[22]Department of Mechanical and Electrical Engineering, Shangdong Management University, Jinan 250357, China.
[23]College of Science, China University of Petroleum, Qingdao 266555, China.
[24]Tokyo Metropolitan College of Industrial Technology, Tokyo 116-8523, Japan.
[25]Department of Physics, Konan University, Kobe 658-8501, Japan.
[26]College of Industrial Technology, Nihon University, Narashino 275-8575, Japan.
[27]Shonan Institute of Technology, Fujisawa 251-8511, Japan.
[28]Research Institute for Science and Engineering, Waseda University, Tokyo 162-0044, Japan.
[29]Japan Atomic Energy Agency, Tokai-mura 319-1195, Japan.
[30]Key Laboratory of Dark Matter and Space Astronomy, Purple Mountain Observatory, Chinese Academy of Sciences, Nanjing 210034, China.
[31]Department of Space Science and Center for Space Plasma and Aeronomic Research, University of Alabama in Huntsville, 320 Sparkman Drive, Huntsville, AL 35899, USA.

Abstract. Cosmic rays do not arrive at the Earth uniformly. Recent experiments have consistently observed small anisotropies with amplitudes of $\sim$0.2% in the arrival directions of cosmic rays at TeV energies. We perform the modeling of the cosmic-ray anisotropy at TeV energies using the intensity-mapping method based on Liouville's theorem. This work indicates unrealistically small-scale ansiotropies with $<\sim 10^\circ$ angular scales in the distribution of the cosmic-ray relative intensity at the outer boundary of the heliosphere. We would possibly need to resolve an issue that the experimental data covers ten years while the Magnetohydrodynamics (MHD) model heliosphere used in this work is only a single snapshot at a certain moment. Performing the intensity-mapping for multiple snapshots of the MHD model heliosphere and taking the average of the results would improve the results of this work.

1. Introduction

Galactic cosmic rays (CRs) do not arrive at the Earth uniformly. Anisotropies with amplitudes of roughly 0.2% have been observed at tera-electronvolt (TeV) energies by recent cosmic-ray experiments (e.g. [1, 2, 3, 4, 5, 6]), such as a large-scale deficit region named 'Loss-Cone' and a large-scale excess region named 'Tail-In'. The origins of these anisotropic features have yet to be revealed, although the anisotropy reflects the propagation of CRs in the magnetic fields of the heliosphere and the surrounding interstellar medium.

Previous papers [7, 8] utilize the 'intensity-mapping' method, in which a model heliosphere is reconstructed by Magnetohydrodynamics (MHD) simulations, CR trajectories in the magnetic fields of the MHD model heliosphere are calculated, and Liouville's theorem is employed to map the distribution of the CR intensity at the Earth to the outer boundary of the heliosphere. Then, the obtained anisotropies of the CR intensity at the outer boundary is interpreted in physical terms by modeling the intensity distribution based on a superposition of CR flows. It was indicated in the previous paper [7] that, dominant in the interstellar medium outside the heliosphere is a dipole flow of CRs along the interstellar magnetic field ($B_{\rm ISM}$), and that a density gradient of CRs also exists in the direction of the Vela supernova remnant.

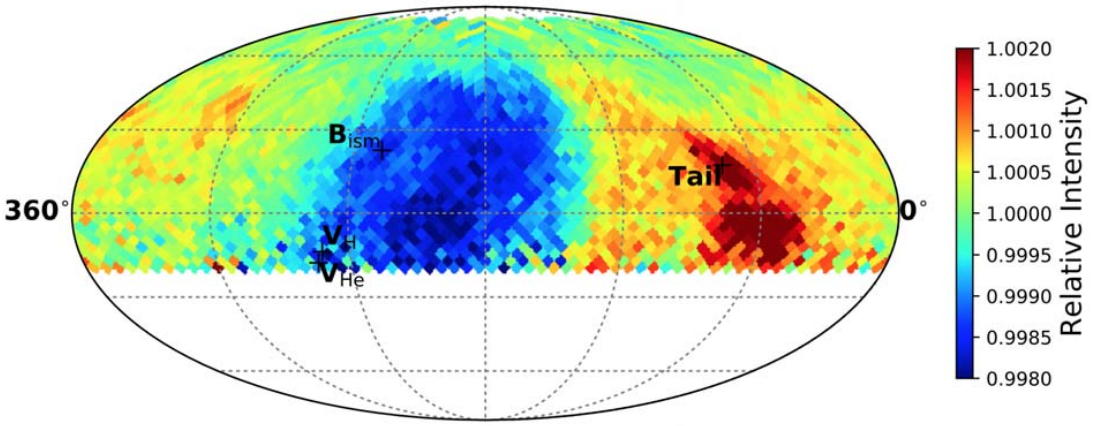

Figure 1. CR relative intensity ditribution in equatorial cooridnates obtained from the data of the Tibet ASγ experiment taken from November 1999 to May 2010.

In order to make the modeling conclusive, however, two technical issues must be resolved. Firstly, the previous work [7] employed protons with monochromatic energy of 4 TeV for the intensity-mapping, although the energy change of those protons due to the acceleration and deceleration in the MHD model heliosphere were taken into account. Since CRs arriving at the Earth are composed of different atomic nuclei with different energies, the energy spectrum and the composition of observed CRs must be taken into account in the intensity-mapping process. Secondly, the χ^2/d.o.f. of the fitting between the experimental data and the best-fit model anisotropy was 4.5 in the previous paper, which was not good enough. The χ^2/d.o.f. value must be reduced to ~ 1 by improving the modeling of the distribution of the CR intensity at the heliospheric outer boundary.

2. Intensity Mapping

In this work, we use the data obtained from November 1999 to May 2010 by the Tibet ASγ experiment. Figure 1 shows the obtained CR relative intensity distribution in equatorial coordinates. We pixelize the sky in our field of view ($-20^\circ <$ decl. $< 80^\circ$) in 2056 pixels, using the HEALPix algorithm [9] with $N_{\rm side} = 16$. Each pixel has an approximate size of $3.7^\circ \times 3.7^\circ$. We estimate the rigidity distribution of observed CRs using detailed Monte Carlo (MC) simulations of air-shower generation and detector response. We generate air showers using CORSIKA v7.4000 [11] with EPOS LHC [12] for the high-energy hadronic interaction model and FLUKA v2011.2b [13, 14] for the low-energy hadronic interaction model, in the energy range from 0.3 TeV to 10 PeV based on a model of the CR energy spectrum and chemical composition derived from direct measurements [10]. We feed the generated air showers into the detector response simulation developed by GEANT v4.10.00 [15] and analyze them in the same way as the experimental data. The obtained rigidity distribution of CRs is shown in Figure 2 for three declination bands.

We use the fourth-order Runge-Kutta method to calculate the trajectories of CRs in the MHD model heliosphere. To smooth out possible seasonal effects, we place the Earth at four positions on the ecliptic plane at a distance of 1 AU from the Sun. Using the HEALPix algorithm [9] we pixelize the sky with $N_{\rm side} = 32$ in the declination range from -20° to 80°, and shoot CR anti-partiles from each pixel center into the MHD model heliosphere, sampling their rigidity

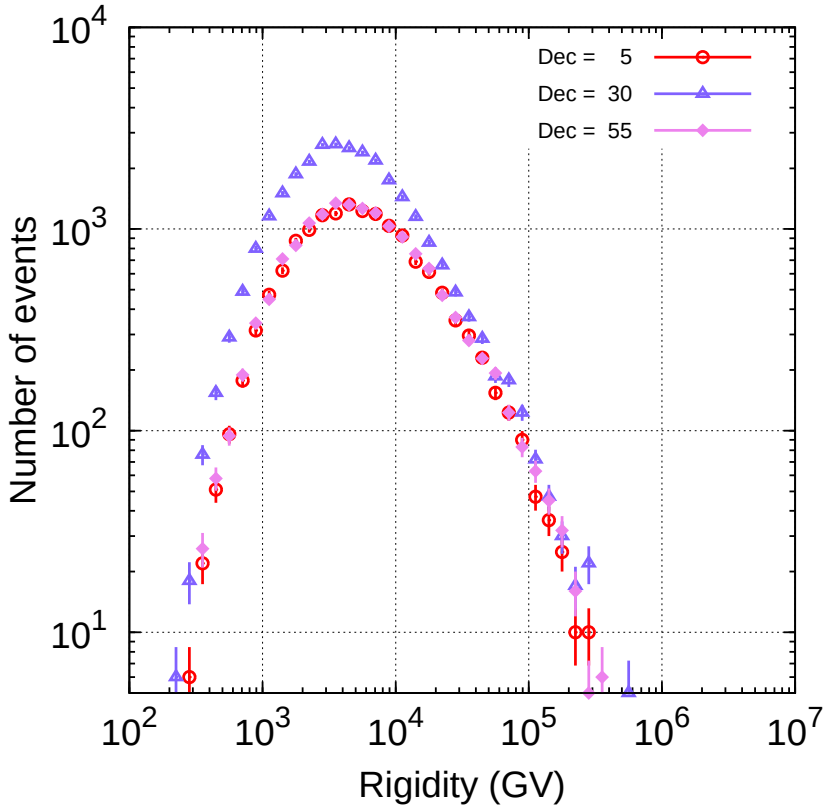

Figure 2. Distribution of CR rigidity as seen by the Tibet ASγ experiment for three declination bands, reproduced with detailed MC simulations.

from Figure 2. We use the same MHD model heliosphere as the one employed in [7]. We track the CRs in the MHD model heliosphere and record their momentum directions at the outer boundary, and then the CR intensity at the outer boundary in the CR momentum direction ($I_{\rm ISM}$) is regarded as equal to that at the Earth ($I_{\rm E}$). We evaluate the distribution of the relative intensity of CRs at three boundaries at distances of 630 AU, 1580 AU and 3980 AU from the Sun, with the nose direction truncated at the surface where the direction (strength) of the magnetic field becomes different from that outside the heliosphere by $< 0.1^\circ$ (0.1%).

The 'declination bias' exists in the experimental data —- the average of the CR intensity has been normalized to unity in each declination band since the detection efficiency of the experiment has not been absolutely calibrated along declination. The following steps, therefore, need to be taken to estimate the $I_{\rm ISM}$ distribution at the outer boundary: 1) construct $I_{\rm ISM}$, a model of the CR intensity distribution at the outer boundary, 2) map $I_{\rm ISM}$ to that at the Earth $I_{\rm E}$ based on the CR trajectory calculation in the MHD model heliosphere, 3) normalize the average of $I_{\rm E}$ to unity in each declination band, and 4) obtain χ^2 between the experimental data and the normalized $I_{\rm E}$. We repeat these four steps until the χ^2 is minimized, and obtain the best-fit model of $I_{\rm ISM}$. We express the distribution of the CR relative intensity at the outer boundary in spherical harmonics Y_{lm} at step 1):

$$I_{\rm ISM} = 1 + \sum_{l=1}^{l_{\rm max}} \sum_{m=-l}^{l} f_{lm} Y_{lm} + I_{\rm CG}, \tag{1}$$

where f_{lm}'s are free fitting parameters. We increase the maximum order $l_{\rm max}$ of the spherical harmonics until we get the χ^2/d.o.f. close to unity.

3. Results and Discussions

The results are summarized in Figure 3. Panels (a), (b) and (c) are the best-fit model distributions of the CR relative intensity at the outer boundaries at distances of 630 AU, 1580 AU and 3980 AU from the Sun, respectively. The maximum order $l_{\rm max}$ of the spherical harmonics Y_{lm} in Eq.(1) is $l_{\rm max} = 4$ for Panel (a), $l_{\rm max} = 8$ for Panel (b), and $l_{\rm max} = 20$ for Panel (c), and the obtained χ^2/d.o.f. values are 0.96 (probability 89%), 0.98 (71%) and 0.94 (95%), respectively. From Figure 3, one can notice that $l_{\rm max}$ decreases as the distance of the boundary from the Sun decreases. In terms of physics, it should be a natural assumption that only large-scale anisotropies exist in the distribution of the CR intensity at the helisopheric outer boundary, and that small-scale anisotropies are added to the intensity distribution by the modulation of CR trajectories in the heliospheric magnetic field. The tendency seen in panels (a) – (c) in Figure 3, however, disagrees with this assumption. Considering that the MHD model heliosphere employed in this work has been refined already to give reasonable agreement with experimental results (for details see [7]), we consider that our intensity mapping needs to be improved further. One possible issue would be that, the CR scattering with magnetic irregularities in the heliosphere is not taken into account in the intensity mapping process when we calculate CR trajectories in a single snapshot of the magnetic field structure of the MHD model heliosphere, while the experimental data used in this work, covering a period of ∼ten years, contains this CR scattering effect. This discrepancy would be resolved by performing the intensity-mapping for multiple snapshots of the MHD model heliosphere and taking the average of the results, which would lead to remove the unnatural tendency in Figure 3 and enable us to derive CR flows in the interstellar medium outside the heiosphere.

Acknowledgments

The collaborative experiment of the Tibet Air Shower Arrays has been conducted under the auspices of the Ministry of Science and Technology of China and the Ministry of Foreign Affairs

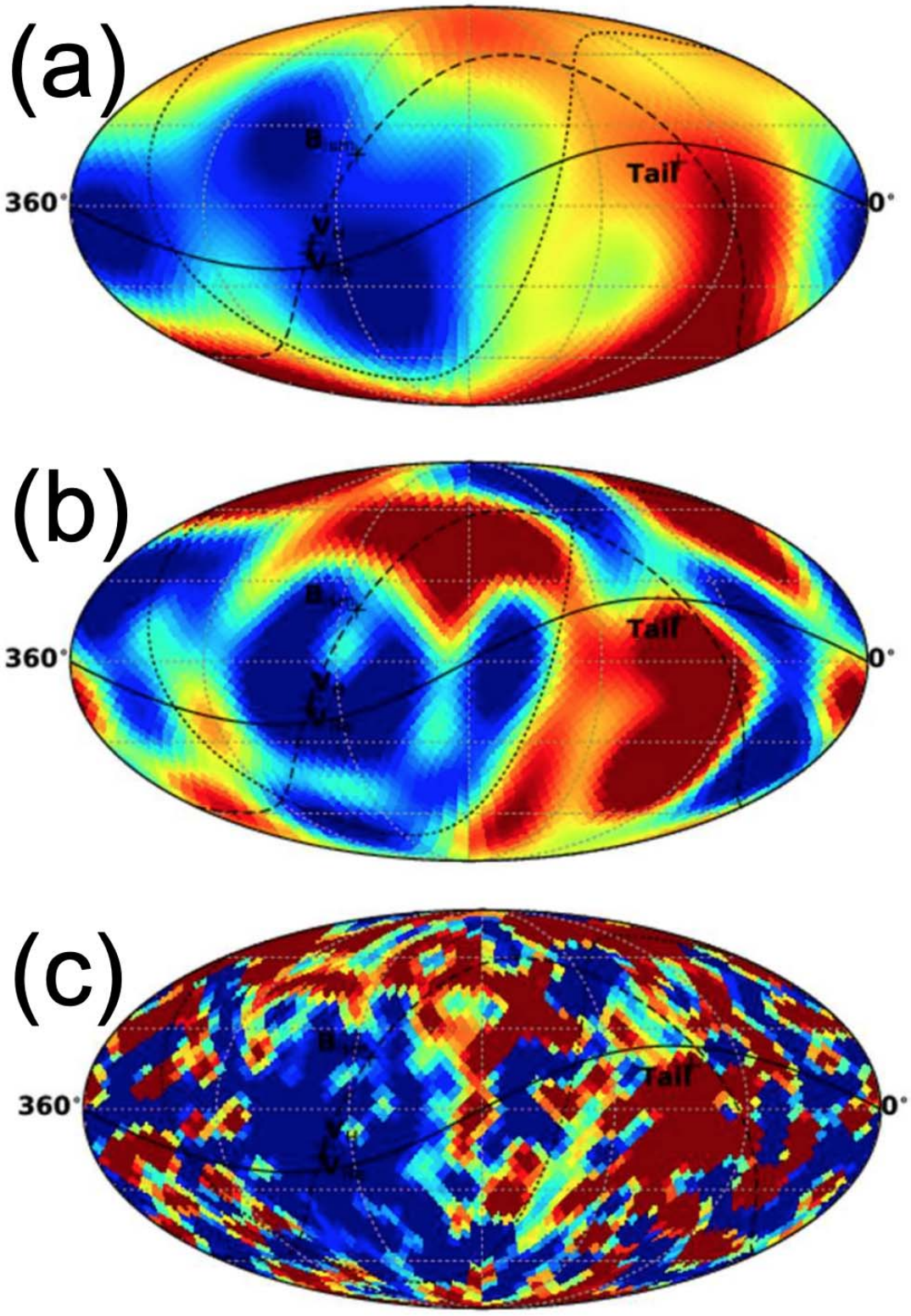

Figure 3. Best-fit model distributions of the CR relative intensity at the heliospheric outer boundaries at distances of 630 AU (a), 1580 AU (b) and 3980 AU (c) from the Sun, respectively.

of Japan. This work was supported in part by a Grant-in-Aid for Scientific Research on Priority Areas from the Ministry of Education, Culture, Sports, Science and Technology, and by Grants-in-Aid for Science Research from the Japan Society for the Promotion of Science in Japan. This work is supported by the National Natural Science Foundation of China under Grants No. 12227804, No. 12275282 and No. 12073050, and the Key Laboratory of Particle Astrophysics, Institute of High Energy Physics, CAS. This work is also supported by the joint research program of the Institute for Cosmic Ray Research (ICRR), the University of Tokyo.

References

[1] A. U. Abeysekara *et al.*, Astrophys. J., **871**, 96 (2019)
[2] A. U. Abeysekara *et al.*, Astrophys. J., **865**, 57 (2018)
[3] M. G. Aartsen *et al.*, Astrophys. J., **826**, 220 (2016)
[4] B. Bartoli *et al.*, Astrophys. J., **809**, 90 (2015)
[5] M. Amenomori *et al.*, Astrophys. Space Sci. Trans., **6**, 49 (2010)
[6] M. Amenomori *et al.*, Science, **314**, 439 (2006)
[7] M. Zhang *et al.*, Astrophys. J., **889**, 97 (2020)
[8] M. Zhang *et al.*, Astrophys. J., **790**, 5 (2014)
[9] K. M. Górski *et al.*, Astrophys. J., **622**, 759 (2005)
[10] M. Shibata *et al.*, Astrophys. J., **716**, 1076 (2010)
[11] D. Heck *et al.*, CORSIKA: a Monte Carlo Code to Simulate Extensive Air Showers Report FZKA-6019 (Forschungszentrum Karlsruhe, 1998)
[12] T. Pierog *et al.*, Phys. Rev. C, **92**, 034906 (2015)
[13] A. Ferrari *et al.*, Report CERN-2005-10, INFN/TC_05/11, SLAC-R-773 (CERN European Organization for Nuclear Research, 2005)
[14] T. T. Böhlen *et al.*, Nucl. Data Sheets, **120**, 211 (2014)
[15] S. Agostinelli *et al.*, Nucl. Instrum. Meth. A, **506**, 250 (2003)